HEFAT2014
10th International Conference on Heat Transfer, Fluid Mechanics and Thermodynamics
14 – 16 July 2014
Orlando, Florida

NUMERICAL MODELING OF DEMISTER IN MULTI STAGE FLASH (MSF) DESALINATION

Obeid F., Janajreh I.* and Chaouki Ghenai
*Author for correspondence
Department of Mechanical Engineering,
Masdar Institute,
Abu Dhabi,
United Arab Emirates,
E-mail: ijanajreh@masdar.ac.ae

ABSTRACT

In this work, the water vapor flow across a demister in a flash chamber is simulated. An important desirable feature of a demister is low pressure drop and high separation efficiency. Thus the pressure drop of a demister is analyzed with variations in channel velocity magnitude, channel velocity profile and viscous and inertial resistance to determine their effects. The effect of demister wire diameter on performance is also studied. Results obtained from Computational Fluid Dynamics (CFD) modelling are validated using experimental data and/or empirical correlation available in the literature.

INTRODUCTION

Desalination involves removal of salt from seawater to make it suitable for human consumption, utilization and water irrigation etc. There are various methods adopted in desalination and they could be broadly categorized into thermal and membrane desalination processes. Thermal desalination processes include Multi Stage Flashing (MSF), Multiple Effect Evaporation (MED) and Single Effect Evaporation (SED). The MED is made up of two main systems namely Mechanical Vapor Compression (MVC) and Thermal Vapor Compression (TVC). Membrane desalination processes include Reverse Osmosis (RO), Direct Contact Membrane Desalination (DCMD) and Electro Dialysis (ED). In RO and DCMD fresh water permeates through a semi-permeable membrane under high and low pressures respectively, while leaving behind water with high brine concentration. In ED, electrically charged salt ions are separated through ion exchange membranes to leave a water product without salinity. A schematic diagram of the conventional desalination processes is presented in Figure 1. According to Krishna [1], about 50% of world's desalination is provided by distillation processes of which MSF constitutes 84%. When MSF was initially adopted around 1960's, there was the problem of frequent contamination of distillate product and fouling of the condenser at a very rapid rate. With the introduction of demisters (mist separators), the problem was overcome.

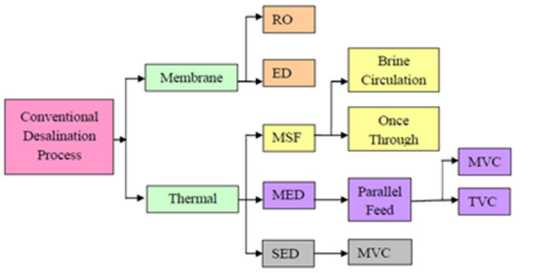

Figure 1: Conventional desalination processes

NOMENCLATURE

A_s	[m²/m³]	Specific area
C_p	[J/kg°C]	Specific heat at constant pressure of water
C_{pv}	[J/kg°C]	Specific heat at constant pressure of steam
d_p	[mm]	Maximum diameter of the captured droplets
d_w	[mm]	Diameter of the wire
d_i	[m]	Column inside diameter
L	[mm]	Packing thickness
V	[m/s]	Vapour velocity
ρ_l	[kg/m³]	Liquid density
ρ_v	[kg/m³]	Vapour density
k		Constant
P	[Pa]	Pressure
ρ	[kg/m³]	Density
μ	[W/m³]	Molecular viscosity
u'_i		Velocity fluctuations
$\overline{u}$		Average velocity

x_i	Cartesian coordinates in the x, y and z directions
t	Time increment
u_i	Velocity component in x_i direction
g_i	Gravitational acceleration components
τ_{ij}	Stress tensor components

A demister is a device often fitted to separate trapped and entrained liquid bobbles in the vapor stream. Demisters may be a mesh type coalesce, vane pack or other structure. The mesh demister, Figure 2, consists of mats made up of many layers of wire mesh (a simple porous blanket of metal wire that retain liquid droplets entrained by the water vapor), each staggered relative to the next. These mats are placed horizontally facing the stream of vertically rising vapor. As the vapor rises, the entrained droplets collected on mesh wires, merge into larger drops and drip from the bottom layer. Separators of this design present very little resistance to vapor flow and enable production of distillate with as low as 0-5ppm salinity[2].

Demisters can reduce the residence time required to separate a given liquid droplet size, thereby reducing the volume and associated cost of separator equipment. Wire mesh demister performance depends on many variables including: support grids, vapor velocity, wire diameter, packing density, pad thickness and material of construction. Since the wire-mesh is not rigid, it must be supported on suitable grids. To obtain the least pressure drop, maximum throughput and maximum efficiency, the support grids must have a high percentage of free passage. Even with the development and success recorded with demisters, the design and installation of demisters is poorly understood. Recent studies of Al-Fulaij et al. [3] and Janajreh et al. [4] have added to the understanding of demisters and their design.

Demisters use a combination of inertial impaction, direct interception and Brownian motion mechanisms to remove mist from distillate [5]. Some experimental work include El-Dessouky et al. [5] and Helsør and Svendsen [6]. Janajreh et al. [4] inferred from conducted experimental studies and their simulation that increase in the vapor velocity and droplet size increases separation efficiency. Flooding and loading velocities increase with decrease in packing density and increase in wire diameter. They also stated that while the specific pressure drop for a dry demister is low, it has a higher rate of increase in a wet/flooded demister. In both cases, the specific pressure drop increases with increase in vapor velocity.

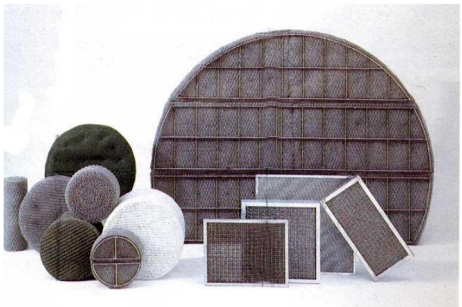

Figure 2: Wire mesh demister

Modelling and simulation are also used in improving demister performance. Rosso et al. [7] developed a steady-state mathematical model to analyze MSF desalination process. The model accounts for various parameters such as stages geometry, variation of physical properties of water with temperature and salinity and the mechanism of heat transfer. They used the model to study the effect of number of stages, sea water temperature and steam temperature on the desalination process.

Using computational fluid dynamics (CFD), Abdel-Jabbar et al. [8] modelled and simulated performance characteristics of large scale MSF plants. They analyzed design parameters including weir loading, dimensions of condenser tube bundle, demister dimensions, stage dimensions and temperature considering the large size of the plant. They found out that system design strongly depends on capacity and stage width. Mansour and Fath [9] developed CFD model based on Ansys/Fluent to determine the optimum position and number of jumping plates (wire) in an MSF flash chamber to enhance thermal properties. They concluded that using a single jump plate located at the middle of the chamber gives higher thermal efficiency to the flashing process. Rahimi and Abbaspour [10] used FLUENT to obtain the pressure drop across a wire mesh mist eliminator as a function of vapor velocity, packing density and wire diameter. Their results matched both experimental and empirical data.

Al-Fulaij et al. [3] were motivated by the poor understanding of demister design and installation in the literature to design a new demister. They emphasized on the wire diameter and stage temperature to achieve optimal performance. A demister with the same dimensions was analyzed for different wire dimensions and an optimum diameter of 0.24 mm was preferentially chosen over 0.20 mm and 0.28 mm because it gave a low pressure drop without compromising separation efficiency. Janajreh et al. [4] added to the understanding of demisters by simulating the vapor water flow across a demister while considering real demister dimensions. The demister was modelled as porous medium. The effect of velocity profile, viscous and inertial resistance on pressure drop was determined. Viscous and inertial resistances were found to be the parameters with the most effect on pressure drop.

On the other hand, a limited number of literature studies are found on demister performance evaluation. Research on evaluation of the performance of the wire mesh mist eliminator in operating conditions of MSF plants is still in an immature state. The available theoretical models devoted to simulation of the performance of the wire mesh pads are not adequate for implementation to industrial units [5]. Due to complexity of the problem, most of the previous work was empirical. The common design procedure for vapor release velocity and the vapor velocity within the demister which according to the Souders-Brown relation, is given by:

$$Vmax = K\sqrt{\frac{\rho l - \rho v}{\rho v}} \quad (1)$$

Where K is a constant which depends on the de-entrainment height and on the physical properties of the working fluids. Values are reported equal to 0.058 and 0.078 for the vapor

release velocity and vapor velocity within the demister, respectively. This method of designing wire mesh separators is very rough and is not practical.

An empirical correlation based on an experiment was developed by El-Dessouky et al. [5] for determination of the removal efficiency of large mist droplets by wire mesh mist eliminator. The demister performance was evaluated by droplet separation efficiency, vapor pressure drop of wet demister, flooding and loading velocities. These variables were measured as a function of vapor velocity, packing density, pad thickness, wire diameter and diameter of captured droplets. This limits the correlation validity to the range of variables covered by the experiments. It was mentioned that in order to prevent any re-entrainment of the water droplets captured in the wire mesh pad, the gas phase velocity should be limited to 4-5m/s. Also, he presented experimental data for the flooding load, the corresponding increase in pressure drop and the fractional separation efficiency.in a dimensionless form, the fractional degree of precipitation depends on the Stokes, the Reynolds and Euler numbers. Experimental analysis shows that for large Reynolds numbers and large range of Euler number, the inertial precipitation depends on a dimensionless precipitation parameter. Therefore, a simple approximation formula is given for the fractional degree of precipitation and the limiting droplet size for all type of separators. A semi empirical model for the demister design, which is built on previous analysis evaluated the inertial capture efficiency for a single wire, expressed in terms of a dimensionless Stoke number. The analysis for industrial wire mesh packing as a function of the demister pad thickness, the demister specific area, and the number of mesh layers. A new model was presented for predicting the removal efficiency of complex wire mesh eliminators. This new model can be used for predicting separation efficiency for multilayer pads and composite separators. Recently, a limited number of research has tackled the demister modelling using computational fluid dynamics (CFD). For the wire mesh demisters, Rahimi and Abbaspour [10] studied the pressure drop in a mist pad by (CFD). The turbulence models based on the standard k-ε model was used to simulate the measurements of the pressure drop and was carried out for inlet velocity ranging 1-7m/s. The CFD predictions were conforming to the experimental data and El-Dessouky et al. [5] empirical correlation. Also, the simulations show existence of a maximum in separation efficiency as a function of the vapor inlet velocity. This indicated that further increase in the velocity will result in droplet re-entrainment and carryover of fine droplets in the vapor stream.

The separation processes in the wire mesh demisters undergo the following three successive steps, which are illustrated in Figure 3 [5]; 1) Accumulation through which the mist impact the wire with a tendency to wet and stick to the surface. The contact usually creates a thin liquid film on the wire.

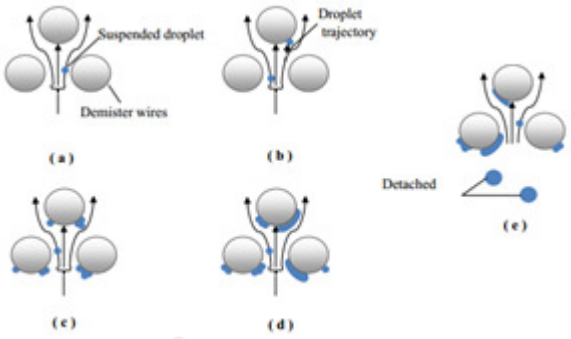

Figure 3: Steps of water droplets separation from vapour stream in the mesh demister (a) clean wire mesh, (b) accumulation, (c) and (d) coalescence, (e) detachment [5]

Depending on the size of the wire, this thin film may either break up into smaller drops if the wire is small, or it may grow into a ligament hanging beneath the wire if the wire is large. 2) Coalescence of the droplets which impinging wire surface to form larger size drops. In the momentum induced dripping mode, when the incoming droplets make contacts with the wire, a water film builds up consistently. The film runs off the contact point and wraps around the wire from both sides and finally the film reattaches and forms a large fragment beneath the wire. 3) Detachment of the liquid drops drain back from the upstream face of the wire mesh pad during the vertical flow configuration. In the horizontal flow systems, collected liquid droplets drain down through the vertical axis of the mesh pad in a cross flow fashion. As the fragment becomes larger, it wriggles more vigorously under the influence of gravity as well as the momentum added by the impacting droplets. Finally, the surface tension at the interfacial contact can no longer sustain the combined effect of the weight, and the downwards force of the impacting drops on the ligament.

This work seeks to verify the simulation of Janajreh et al. [4] using the same MSF plant dimensions and CFD tool, FLUENT. The dimensions are based on Sidi-Krir desalination plant in Alexandria, Egypt. It aims to improve the understanding of the design and installation of demisters as by Al-Fulaij [3]. The water vapour flow across a demister in a flashing chamber will be simulated as a porous medium using the CFD tool FLUENT. The understanding of pressure drop across the demister and its design parameters will be considered. The effect of channel velocity magnitude, channel velocity profile, viscous and inertial resistance on pressure drop will be analysed. The simulation will be validated using empirical correlation and/or experimental data available in literature.

NUMERICAL METHOD

The dimensions and values of parameters are based on a real plant Sidi-Krir desalination plant in Alexandria, Egypt. The flow across the demister can be modelled as porous jump, porous medium or by direct numerical simulation. Porous jump does not consider the demister thickness and is more fit for thin screen

structure than real demister. In direct numerical simulation, the dense grid and high resolution required, makes it computationally very expensive. Compromising between accuracy and cost, the option would be to model the demister as a porous medium.

The geometry of the flash chamber including the demister used for computation is presented in Figure 4 and Table 1. The dimensions are based on the Sidi-Krir desalination plant. The geometry also indicates the boundary conditions used after meshing.

MODEL GOVERNING EQUATIONS

In modelling the demister as a porous medium, the flow is governed by Navier-Stokes equations. The three dimensional transient incompressible Navier Stokes equations are employed after adjusting them for turbulence using the k-ε model and accounting for the flow within the demister as a porous media. The equations after averaging are given by:

Continuity:

$$\frac{\partial \bar{\rho}}{\partial t} + \frac{\partial \overline{\rho u_l}}{\partial x_i} = 0 \qquad (2)$$

Momentum:

$$\frac{\partial \overline{\rho u_l}}{\partial t} + \frac{\partial (\overline{\rho u_l u_j})}{\partial x_j} = \frac{\partial \tau_{ij}}{\partial x_i} + \bar{\rho} g_i \qquad (3)$$

Constitutive:

$$\tau_{ij} = -\bar{\rho}\delta_{ij} + \mu\left(\frac{\partial \overline{\rho u_l}}{\partial x_j} + \frac{\partial \overline{\rho u_j}}{\partial x_i}\right) - \overline{\rho u_l' u_j'} \qquad (4)$$

S_i is the momentum sink that is activated for the porous media

$$\frac{\partial \overline{\rho u_l}}{\partial t} + \frac{\partial (\overline{\rho u_l u_j})}{\partial x_j} = \frac{\partial \tau_{ij}}{\partial x_i} + \bar{\rho} g_i + S_i$$

Where the source term S_i is given by:

$$S_i = \sum_j^3 D_{ij} \mu v_j + \frac{1}{2} \sum_j^3 C_{ij} \rho |v| v_j \qquad (5)$$

Furthermore the flow in porous media is governed by the same equations 2 and 3 subjected to porosity coefficient (γ) multiplication. γ is defined as the as the ratio of volume of the void to the total volume. The pressure gradient in the porous cell is affected by the sink and the pressure gradient proportional to the square of velocity is created. When the medium is homogeneous Eq. 5 becomes:

$$S_i = -\left(\frac{\mu}{\alpha} v_i + \frac{1}{2} C_2 \rho |v| v_i\right) \qquad (6)$$

Where α is the permeability and C_2 is the inertial resistance factor. In fluent, D and C are specified as diagonal matrices with 1/α and C_2, respectively, on the diagonals and other elements are zeroes. In the current analysis α for the demister is represented by 0.984 porosity, and with a permeability value, α , of 1.95e-06 m_2 and inertia resistance value, C_2, of 209.9m^{-1}. These equations are subjected to inlet velocity, out flow pressure, and wall boundary conditions as depicted in figure 4.

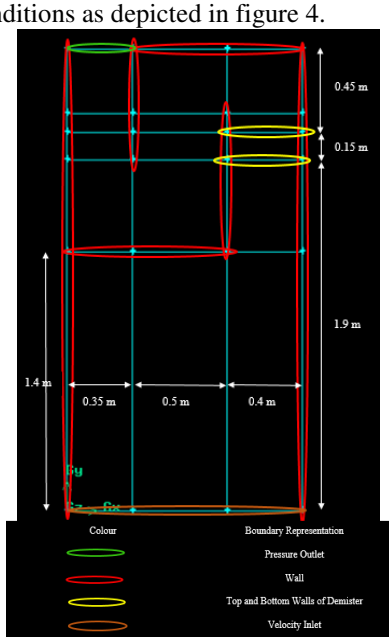

Figure 4: Geometry of a single flash chamber

Table 1: Properties of demister and flashing chamber

Flashing Chamber	
Inlet Velocity	0.72 m/s
Inertial Resistance	209.9 m-1
Viscous Resistance	512820 m-2
Fluid and Fluid Density	Single Phase – Water Vapour: 0.5542 kg/m3
Demister Thickness	0.15m
Gauge Pressure	0.1 MPa
Demister	
Height	0.15m
Wire Diameter	0.28mm
Packing Density	125.8 kg/m3
Surface Area	224m2/m3
Porosity	0.984

SIMULATION ASSUMPTION AND SETUP

Considering the given geometry in Figure 4 and the governing equations, the flow is assumed to be two-dimensional, steady state, isothermal and incompressible. An implicit pressure-based solver is issued. The k-ε model is used for turbulence modelling with default coefficients are given in FLUENT. The fluid is assumed to have a single phase (water vapor) with density of 0.5542kg/m^3 and viscosity 1.34e^{-5}kg/ms. The simple solution scheme is used for pressure with standard

first order. For momentum and turbulent kinetic energy, second-order upwind is used and for turbulent dissipation rate, first order upwind is used.

The mesh was generated using multiple block and Cartesian type with total 58,166 cells. As shown in Figure 5, the boundary mesh was used at walls of the flash chamber and demister.

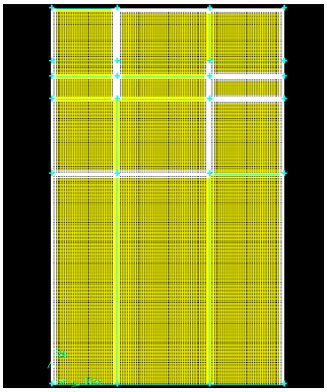

Figure 5: Mesh of single flash chamber in Gambit

The turbulent scalars, i.e. turbulent kinetic energy (k) and turbulent dissipation rate (ε) are written as:

$$\rho u_i \frac{\partial k}{\partial x_i} = \mu_t \left(\frac{\partial u_j}{\partial x_i} + \frac{\partial u_i}{\partial x_j} \right) \frac{\partial u_j}{\partial x_i} + - \frac{\partial}{\partial x_i} \left(\frac{\mu_t}{\sigma_k} \frac{\partial k}{\partial x_i} \right) - \rho \varepsilon$$

$$\rho u_i \frac{\partial \varepsilon}{\partial x_i} = C_{1\varepsilon} \frac{\mu_t \varepsilon}{k} \left(\frac{\partial u_j}{\partial x_i} + \frac{\partial u_i}{\partial x_j} \right) \frac{\partial u_j}{\partial x_i} + \frac{\partial}{\partial x_i} \left(\frac{\mu_t}{\sigma_\varepsilon} \frac{\partial \varepsilon}{\partial x_i} \right) - C_{2\varepsilon} \frac{\rho \varepsilon^2}{k}$$

(6)

The right hand terms represent the generation, the diffusion and the destruction, respectively. In these equations, μ_t is the turbulent or eddy viscosity $\mu_t = f_\mu C_\mu \rho k^2 / \varepsilon$ where f and C along with $C_{1\varepsilon}$, $C_{2\varepsilon}$, σ_k and σ_ε are empirical constants.

PROCESSING OF RESULTS

Using the pressure drop across the demister for a constant inlet velocity of 0.72 m/s. From Figure 6 and 7, the contours of static pressure present in the case where there is a demister and without demister. In Figure 6a the pressure varies between 94 Pa and 115 Pa. In Figure 7a, before reaching the demister, the pressure remained almost constant. However, after reaching the demister, the pressure dropped and the vapour flow proceeded. The pressure drop is shown in Figure 8 for the cases without porous/ demister and with demister. The velocity is visibly lower in the case where demister is present.

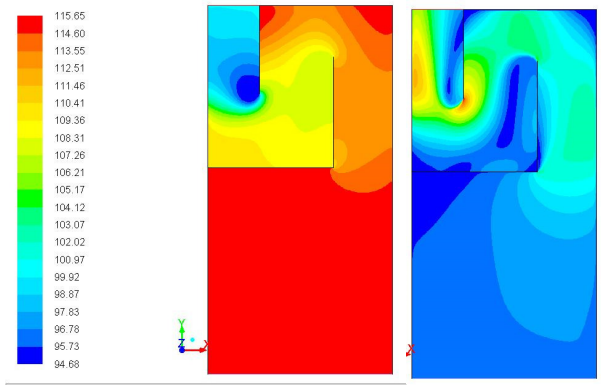

Figure 6: a) Simulation of flow without using porous medium- pressure contours, b) Simulation of flow without using porous medium- velocity magnitude

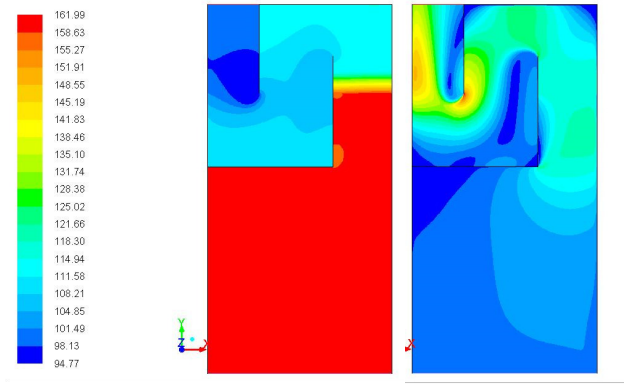

Figure 7: Simulation of flow across demister using porous medium- pressure contours; b) Simulation of flow across demister using porous medium- velocity magnitude

As shown in Figure 8b, the pressure at the bottom of the demister is higher than the pressure at the top. The pressure drop across the demister is 45 Pa. This value is very similar to that obtained by Janajreh et al. [4]. To further verify and validate the results, theoretical and empirical values will be used.

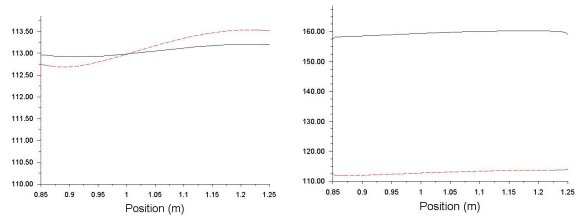

(a) (b)

Figure 8: a)Pressure drop in MSF chamber – without demister b) Pressure drop in MSF chamber with demister

COMPARISON OF RESULTS WITH EXPERIMENTAL DATA

Ergun's equation can be used to calculate the pressure drop. It is given by:

$$\frac{\Delta P}{L} = \frac{150\mu}{D_p^2}\frac{(1-\varepsilon)^2}{\varepsilon^3}v_\infty + \frac{1.75\rho}{D_p}\frac{(1-\varepsilon)^2}{\varepsilon^3}v_\infty^2 \quad (7)$$

The variables are defined in Table 2.

Table 2: Pressure drop using Ergun equation [4]

Porosity	ε	0.984
Mean particle diameter (m)	D_p	0.00028
Inertial Loss (m^{-1})	C_2	209.9
Medium permeability (m^2)	α	1.95e-06
Thickness (m)	L	0.15
Laminar fluid viscosity (kg/ms)	μ	1.34e-05
Velocity normal to porous face (m/s)	V	2.51
Density (kg/m^3)	ρ	0.5542
Erugen pressure drop (Pa)	ΔP	57.563
Result from simulation	ΔP	45.81467
% Difference from simulated	% Difference	-20.4

The percentage difference in pressure drop given is relative to the CFD simulation. From Svendsen's empirical data, pressure drop could be also computed. Svendsen's empirical relation is given by:

$$\frac{\Delta P}{h} = \beta_1 U + \beta_2 U^2 \quad (8)$$

Where $\beta_1 = \frac{\mu}{K}$ and $\beta_2 = C_p$

Svendsen used a least square regression. The values of K and C_p are obtained from regression analysis with a confidence interval of 95%. The values are K=2.6e^7 and C=43 [4].

Table 3 presents the pressure drop as well as velocity computed at inlet from computation of various inlet velocities corresponding to different stages in the flash chamber (FC). The desalination plant under consideration has 20 FC stages and as expected, with the increase in FC stage, the velocity decreases. The same trend is seen from all results. However, there is a deviation between the simulated values and experiments and theory. This might be due to some modelling deficiencies in vortex formulation, flow regime and turbulence which are not well accounted for in Janajreh et al. [4] study. We are also considering only one phase when in reality it is a two-phase flow and after the demister, there is condensation. All these are not considered and are potential sources of errors. As compared with the simulation by Janajreh et al. [4]. Table 3 shows that the pressure drops closely match but there is an underestimation of velocity. This might arise from minor set-up differences. Generally, the deviation from experiments does not go above 22%. The pressure drops versus inlet velocity are plotted in Figure 9.

Table 3: Pressure drop using Ergun equation [4]

FC #	V_{inlet} (m/s)	$V_{d\text{-}inlet}$ (m/s)	$V_{d\text{-}j}$ (m/s)	ΔP (Pa)	ΔP (Pa)-(J)	ΔP(Pa)-Erugen (% difference)	ΔP(Pa)-Svendsen (%difference)
20	0.441	1.40	1.53	18	17.74	22.01 (18.2%)	20.20 (10.9%)
15	0.543	1.70	1.90	26	26.46	33.46 (22.3%)	27.59 (5.8%)
10	0.619	1.92	2.15	34.25	34.14	42.55 (19.5%)	33.14 (3.4%)
5	0.660	2.05	2.31	38	38.64	48.95 (22.4%)	36.93 (2.9%)
1	0.720	2.25	2.51	45	45.81	57.56 (21.8%)	41.92 (7.3%)

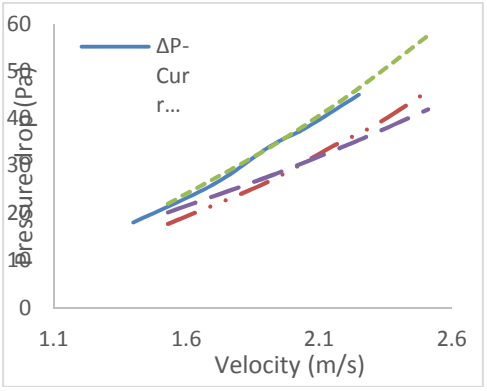

Figure 9: Comparison of pressure drop vs. velocity

DEMISTER CHANNEL VELOCITY PROFILE

The effect of various profiles of inlet velocity was also studied. A constant velocity (0.72m/s), a linear velocity profile and a piece-wise constant and linear velocity were all considered. The results are shown in Figure 10.

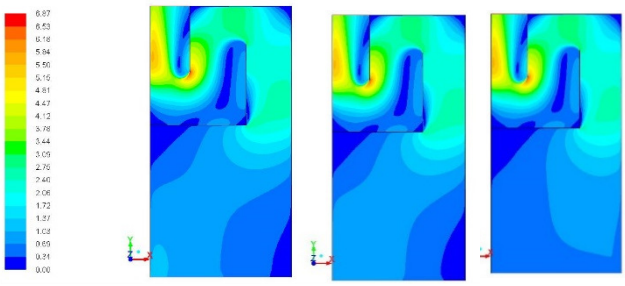

(a) (b) (c)

Figure 10 Velocity contours with varying inlet velocity profile; (a) linear velocity, (b) piece-wise constant and linear, (c) constant velocity

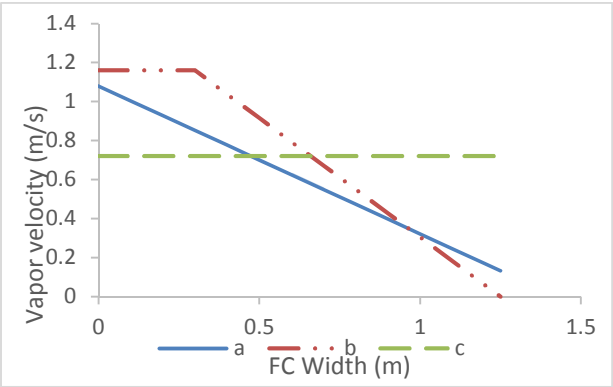

Figure 11: Velocity profiles at inlet; (a) linear velocity, (b) piece-wise constant and linear, (c) constant velocity

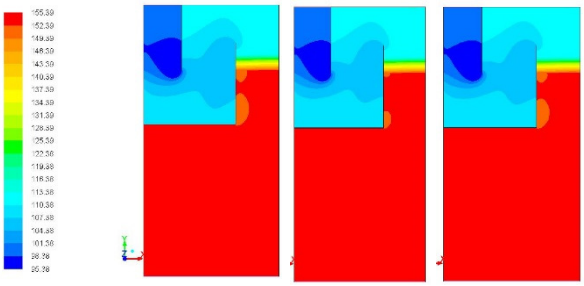

(a) (b) (c)

Figure 12: Pressure contours with varying inlet velocity profile; (a) linear velocity, (b) piece-wise constant and linear, (c) constant velocity

Table 4: Comparison of pressure drops and demister velocities for various velocity profiles

Velocity inlet type	Constant	Linear	Piecewise
Velocity at demister inlet (m/s)	2.25	2.10	2.50
Velocity at demister outlet (m/s)	2.25	2.10	2.50
Pressure drop across demister (Pa)	45.0	41.5	57.5

Table 5: Comparison of pressure drops and demister velocities for various velocity profiles [4]

Velocity inlet type	Constant	Linear	Piecewise
Velocity at demister inlet (m/s)	2.51	2.55	2.63
Velocity at demister outlet (m/s)	2.25	25.25[1]	2.26
Pressure drop across demister (Pa)	45.81	45.70	45.94

The figures and table show the change of velocity magnitude and pressure drops for various inlet velocities. From the current simulation, there seems to be no change in velocity at demister inlet and outlet which seems strange and different from the conclusion of Janajreh et al as seen in Table 5. Though the pressure drop for the constant and linear velocity are quite close, they are different from the profile of the piecewise velocity. Since the profiles are not of exactly the same values, for example the slope in the linear velocity here is higher, this might explain the disparity. The lack of change between inlet and outlet velocity might be due to the choice of location considered as the demister inlet and outlet.

DEMISTER CHANNEL VELOCITY MAGNITUDE

To see the effect of velocity magnitude on the pressure drop, only the demister channel with dimension of 40 cm by 75 cm was considered as shown in Figure 13.

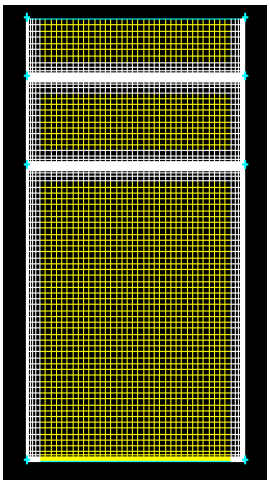

Figure 13: Demister channel mesh

The boundary conditions at the bottom and top are defined as velocity inlet and pressure outlet respectively. The inlet velocity was increased from 1 – 5m/s. As the vapour velocity increases, the pressure drop increases. This trend is the same as seen from all other approaches as compared in Table 6 and Figure 14; all show an exponential trend. The current simulation was in well cohesion with the simulation in [4].

Table 6: Effect of increasing vapor velocity on pressure drop

Vapour velocity (m/s)	ΔP-Current (Pa)	ΔP-Janajreh et al (Pa)	ΔP-Erugen (Pa)	ΔP-Svendsen (Pa)
1.00	9.75	9.6976	14.00257186	11.30535923
1.38	18.00	17.92617	25.64717212	17.47591073
1.93	35.00	34.26806	48.66926354	28.23537491
2.00	36.50	36.72398	52.12269885	29.75989846
2.25	46.00	46.18828	65.42109859	35.49059264
3.00	81.00	81.08179	114.360381	55.36361769
4.00	142.00	142.77355	200.7156182	88.11651692
5.00	225.00	221.79707	311.1884106	128.0185962

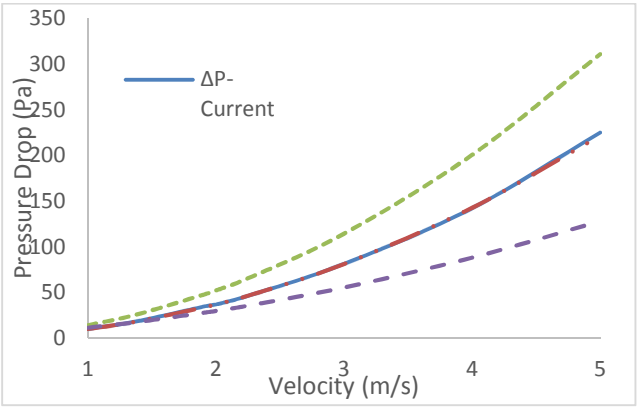

Figure 14: Effect of increasing vapour velocity on pressure drop

Table 7: Pressure drop with the change in inertial resistance

Inertial Resistance (m^{-1})	% Used of base value	ΔP (Pa) Present simulation	ΔP (Pa) [4]	% Change from the pressure drop base value
146.93	70	33	32.7	-30.53
167.42	80	38	37	-20.00
188.91	90	42.5	41.5	-10.53
209.9	100	47.5	45.81	0.00
230.89	110	51	50.1	7.37
251.88	120	56	54.4	17.89
272.87	130	60	58.8	26.32

Table 8: Pressure drop with the change in viscous resistance

Viscous resistance (m^{-2})	% Used of base value	ΔP (Pa) Present simulation	ΔP (Pa) [4]	% Change from the pressure drop base value
398,855	70	46	45.08	-2.65
411,263	80	46	45.31	-2.65
462,671	90	47	45.54	-0.53
512,820	100	47.25	45.81	0.00
565,487	110	47.5	46	0.53
616,895	120	47.5	46.23	0.53
668,303	130	47.5	46.48	0.53

Tables 7 and 8 show the effect of varying inertial resistance and viscous resistance on pressure drop respectively. The reference values are 209.9 m-1 and 512,820 m-2 respectively for inertial and viscous resistance. An increase in viscous resistance has very small effect on the pressure drop while increase in inertial resistance significantly affects the pressure drop. Increasing or decreasing the pressure drop by 30% leads to about 30% change in the inertial resistance. This conclusion is similar to that made by [4].

CONCLUSION

Numerical simulation using CFD (FLUENT) is very important for simulating the flow of vapour across the demister in desalination. The estimated pressure drop was compared with Eurgen's equation, Svendsen's empirical correlation and with work done by Janajreh et al. [4]. Results generally were well agreed with no deviation above 22%. The deviations are due to various simplifications in the model such as single-phase flow and deficiencies in accounting for turbulence, flow regime and vortex formulation. The effect of velocity inlet magnitude, velocity profiles, inertial and viscous resistances were studied. Increase in vapour velocity increases pressure drop exponentially, and change in inertial resistance has a significant effect on pressure drop. While change in viscous resistance has little effect on pressure drop.

Future work will take into account multi-phase flow and condensation that occurs in the flash chamber.

ACKNOWLEDGEMENT

The authors like to acknowledge the class of MEG501 in particular Mr. Gamal and Mr. Isa who helped in running some of the analyses, also Masdar Institute is highly acknowledged for sponsoring this work.

REFERENCES

[1] H. Krishna, "Introduction to Desalination Technologies," pp. 1–7, 1961.

[2] S. Ghani and N. S. Al-Deffeeri, "Impacts of different antiscalant dosing rates and their thermal performance in Multi Stage Flash (MSF) distiller in Kuwait," Desalination, vol. 250, no. 1, pp. 463–472, Jan. 2010.

[3] H. Al-fulaij, A. Cipollina, G. Micale, and D. Bogle, CFD Modelling of the Demister in the Multi Stage Flash Desalination plant, vol. 29. Elsevier B.V., 2011, pp. 1618–1622.

[4] I. Janajreh, a. Hasania, and H. Fath, "Numerical simulation of vapor flow and pressure drop across the demister of MSF desalination plant," Energy Convers. Manag., vol. 65, pp. 793–800, Jan. 2013.

[5] H. T. El-Dessouky, I. M. Alatiqi, H. M. Ettouney, and N. S. Al-Deffeeri, "Performance of wire mesh mist eliminator," Chem. Eng. Process. Process Intensif., vol. 39, no. 2, pp. 129–139, Mar. 2000.

[6] T. Helsør and H. Svendsen, "Experimental Characterization of Pressure Drop in Dry Demisters at Low and Elevated Pressures," Chem. Eng. Res. Des., vol. 85, no. 3, pp. 377–385, Jan. 2007.

[7] M. Mazzotti, M. Morbidelli, M. Rossol, and A. Beltramim, "Modeling multistage flash desalination plants," vol. 108, pp. 365–374, 1996.

[8] N. M. Abdel-Jabbar, H. M. Qiblawey, F. S. Mjalli, and H. Ettouney, "Simulation of large capacity MSF brine circulation plants," Desalination, vol. 204, no. 1–3, pp. 501–514, Feb. 2007.

[9] M. Khamis Mansour and H. E. S. Fath, "Numerical simulation of flashing process in MSF flash chamber," Desalin. Water Treat., vol. 51, no. 10–12, pp. 2231–2243, Feb. 2013.

[10] R. Rahimi and D. Abbaspour, "Determination of pressure drop in wire mesh mist eliminator by CFD," Chem. Eng. Process. Process Intensif., vol. 47, no. 9–10, pp. 1504–1508, Sep. 2008.